Sec61α is required for dorsal closure during *Drosophila* embryogenesis through its regulation of Dpp signaling

Xiaochen Wang and Robert E. Ward IV[1]

Department of Molecular Biosciences, University of Kansas, Lawrence, Kansas 66045

[1]Corresponding author: Robert E. Ward IV, Department of Molecular Biosciences, University of Kansas, 1200 Sunnyside Ave., Lawrence, Kansas 66045

E-mail: robward@ku.edu

Phone: (785) 864-5235

Fax: (785) 864-5294

Running head: *Sec61α* in *Drosophila* embryogenesis

Key words: *Drosophila*, dorsal closure, morphogenesis, *Sec61α*, translocon, *Dpp*, *thick veins*, JNK, cuticle

Grant Sponsor: National Institutes of Health; Grant numbers: R01HD047570 and P20 RR15563

ABSTRACT

During dorsal closure in *Drosophila*, signaling events in the dorsalmost row of epidermal cells (DME cells) direct the migration of lateral epidermal sheets towards the dorsal midline where they fuse to enclose the embryo. A Jun amino-terminal kinase (JNK) cascade in the DME cells induces the expression of Decapentaplegic (Dpp). Dpp signaling then regulates the cytoskeleton in the DME cells and amnioserosa to affect the cell shape changes necessary to complete dorsal closure. We identified a mutation in *Sec61α* that specifically perturbs dorsal closure. *Sec61α* encodes the main subunit of the translocon complex for co-translational import of proteins into the ER. JNK signaling is normal in *Sec61α* mutant embryos, but Dpp signaling is attenuated and the DME cells fail to maintain an actinomyosin cable as epithelial migration fails. Consistent with this model, dorsal closure is rescued in *Sec61α* mutant embryos by an activated form of the Dpp receptor Thick veins.

INTRODUCTION

Dorsal closure is one of the final morphogenetic events necessary for elaborating the body plan of the *Drosophila* larva. Near the midpoint of embryogenesis, immediately after germ band retraction, epidermal tissue covers the ventral and lateral regions of the embryo leaving a large dorsal hole covered only by a squamous extraembryonic epithelium known as the amnioserosa. Coordinated cell shape changes in the absence of cell division in the epidermal cells, coupled with cell shape changes and cell death in the amnioserosa, drive the elongation of the epidermal cell sheets dorsalward, where they meet at the dorsal midline and thereby enclose the embryo.

Dorsal closure in wild type animals involves three distinct stages. Prior to the start of dorsal closure, the cells of the lateral epidermis are polygonal in shape. During the first phase of dorsal closure, known as initiation, the dorsalmost epithelial (DME) cells of the epidermis (also referred to as leading edge cells) elongate in the dorsal-ventral (D-V) axis, whereas the more ventral cells remain polygonal. These DME cells provide an organizing center for the events of dorsal closure. During the initiation phase, the DME cells accumulate actin and myosin in a contractile ring at the level of the adherens junction, which eventually link across these cells to create a continuous actin cable that coordinates the migration of the leading edge of the epithelium (Young et al., 1993). During the second phase of dorsal closure, known as epithelial migration, the more ventral epidermal cells begin to elongate in the D-V axis as the epidermal sheets migrate towards the dorsal midline. This epidermal migration results from the contraction of the actinomyosin cable in the DME cells through a purse string mechanism (Young et al., 1993; Kiehart et al., 2000; Hutson et al., 2003). The actin cable is also necessary to maintain an organized leading front of the DME cells during the migration process (Bloor and Kiehart, 2002; Jacinto et al., 2002). Over the last several years it has become clear that additional forces are contributed by the amnioserosa, which

undergoes coordinated cell shape changes, including contractions perpendicular to the anterior-posterior axis, as well as apical constrictions that eventually lead to those cells being extruded from the epithelium (Kiehart et al., 2000; Harden et al., 2002; Franke et al., 2005; Fernandez et al., 2007). The yolk sac also plays an essential role in these processes as it serves as an attachment substrate for the amnioserosal cells as they contract (Narasimha and Brown, 2004; Reed et al., 2004). Finally, during the completion or zippering phase of dorsal closure, the DME cells meet at the dorsal midline and fuse with DME cells from the contralateral side starting at the anterior and posterior ends and gradually suturing the epidermis towards the center. Again the DME cells show organizing activity by sprouting filopodia and lamellapodia that aid in the alignment and fusion of the two epidermal sheets (Jacinto et al., 2000).

Nearly a hundred genes have been identified whose mutant phenotype includes some defect in dorsal closure. Since it is only the epidermal cells that secrete cuticle late during embryogenesis, a failure to complete dorsal closure produces a characteristic dorsal open phenotype in the resulting dead embryos. Genes that produce this phenotype when perturbed have typically been grouped into two categories, those encoding signaling molecules that are likely required to regulate dorsal closure, and those that encode the cellular effectors of the process. This later class includes cytoskeletal genes such as *zipper*, encoding non-muscle myosin (Young et al., 1993), *myosin phophatase* (Mizuno et al., 2002), *lethal(2)giant larvae*, (Manfruelli et al., 1996) and *chickadee* (Jasper et al., 2001), encoding profilin. Additionally, extracellular matrix genes including the integrin subunits *lethal(1)myospheroid* (Leptin et al., 1989) and *scab* (Stark et al., 1997), also play roles in dorsal closure, as do genes whose products are components of cellular junctions including *armadillo* (Peifer and Wieschaus, 1990), *canoe* (Miyamoto et al., 1995), *coracle* (Fehon et al., 1994), *discs large* (Perrimon, 1988), and *Neurexin* (Baumgartner et al., 1996).

Genetic and biochemical analyses of the genes predicted to encode signaling molecules reveal that although they fall into many classes, they generally impinge on two different conserved signaling pathways, a Jun amino-terminal kinase (JNK) pathway and a transforming growth factor β (TGF-β) pathway (reviewed in Harden, 2002). The JNK pathway is a conserved mitogen activated protein kinase (MAPK) cascade consisting of sequentially acting serine/threonine kinases that lead to the phosphorylation of the transcription factor DJun. DJun then complexes with DFos (encoded by *kayak*), which together make up the adapter protein 1 (AP-1) transcriptional complex (Riesgo-Escovar and Hafen, 1997a). Although JNK signaling is active in both the amnioserosa and the dorsal epidermis during germ band retraction, it is restricted to the DME cells during the initiation of dorsal closure (Reed et al., 2001).

A critical transcriptional target of the JNK pathway in the DME cell is the TGF-β ligand *decapentaplegic* (*dpp*; Glise and Noselli, 1997; Hou et al., 1997; Riesgo-Escovar and Hafen, 1997b). Dpp binds to its receptor, which is a heterotetramer of two type I receptors encoded by *thick veins* (*tkv*) and two type II receptors encoded by *punt* (reviewed in O'Connor et al., 2006). Upon binding of Dpp to its receptor complex, the receptor phosphorylates the SMAD protein Mothers Against Dpp (Mad) that then binds to a co-SMAD named Medea and translocates to the nucleus where it regulates the transcriptional response to the Dpp signal. Mutations in *tkv* and *punt* display dorsal open phenotypes (Affolter et al., 1994; Nellen et al., 1994; Arora et al., 1995). Detailed analysis of the cellular events occurring is *tkv* mutant embryos indicates that Dpp signaling is required for the DME cells to maintain an actinomyosin contractile cable and drive the dorsalward movement of the lateral epidermis, as well as for the cell shape changes in the amnioserosa (Fernandez et al., 2007).

Here we report on the isolation and characterization of a strong loss of function mutation in *Sec61α*, the major subunit of the protein translocon complex for co-translational insertion into the

endoplasmic reticulum. Surprisingly, zygotic loss of *Sec61α* results in specific defects in dorsal closure during mid-embryogenesis. *Sec61α* mutant embryos initiate dorsal closure correctly, as indicated by normal JNK signaling in the DME cells, but cannot generate or maintain a robust contractile actin/myosin cable, and thus fail during the epithelial migration stage of dorsal closure. Strong reductions in the levels of phosphorylated Mad in the lateral epidermis indicate that Dpp signaling is strongly reduced in *Sec61α* mutant embryos. In support of this idea, an activated Tkv receptor provides a highly penetrant, partial rescue of the dorsal closure defects in *Sec61α* mutant animals.

RESULTS

Identification of *Sec61α* alleles

While mapping an EMS-induced mutation recovered from a screen for dominant modifiers of the transcription factor *broad* (Ward et al., 2003), we identified a mutation that failed to complement *Df(2L)BSC6* (cytology 26D3;26F7). We tested loss of function mutations for genes that map to this interval and found that the mutation failed to complement *P{lacW}Sec61α*^{k04917} (Table 1). *P{lacW}Sec61α*^{k04917} (hereafter referred to as *Sec61α*^{k04917}) has a *P*-element inserted into the second intron of the *Sec61α* gene (Fig. 1A). *Sec61α* encodes the major subunit of the tripartite translocon complex required for co-translational insertion of proteins into the endoplasmic reticulum (Johnson and van Waes, 1999). Sequence analysis of genomic DNA isolated from mutant embryos revealed a nonsense mutation in *Sec61α* (G/C to A/T transition at nucleotide 683 of GenBank sequence **AY069569** generating a Trp^{193} to stop mutation; Fig. 1A). We have therefore named this mutation *Sec61α*^{1}. *Sec61α*^{1} is predicted to encode a protein that is prematurely truncated at the end of the fifth of ten transmembrane domains, almost certainly creating a nonfunctional protein (Fig. 1A).

Lethal phase analyses of *Sec61α*^{1} support the molecular analysis and indicate that it is an amorphic allele. Specifically, *Sec61α*^{1}, *Df(2L)BSC6* and *Sec61α*^{1}*/Df(2L)BSC6* mutant animals are completely embryonic lethal, and cuticle preparations of the dead embryos for all of these genotypes showed no ventral denticle belts, differentiated head skeleton or any recognizable cuticle (Table 1 and Figs. 1C, D and data not shown). In contrast, *Sec61α*^{k04917} and *Sec61α*^{1}*/Sec61α*^{k04917} mutant animals showed only ~50% embryonic lethality (Table 1), with the majority of the animals dying in early first instar, suggesting that *Sec61α*^{k04917} is a hypomorphic allele.

Sec61α mutant animals show specific defects in dorsal closure during embryogenesis

Since *Sec61α*^{1} mutant animals have little to no epidermal cuticle, we were able to examine the terminal phenotype of these animals by indirect immunofluorescence using antibodies against Coracle (Cor). Cor is expressed in all ectodermally derived epithelial cells and localizes to septate junctions (Fehon et al., 1994). All late stage 17 *Sec61α*^{1} mutant embryos have no epidermis over the dorsal third of the embryo with the brain and gut extruded through the dorsal hole (Fig. 2B), indicating a completely penetrant defect in dorsal closure. There is little variability in this terminal phenotype as we never observed dorsally closed or partially closed mutant embryos. *Sec61α*^{1}*/Df(2L)BSC6* mutant embryos showed identical phenotypes in both penetrance and expressivity (Fig. 2C). Interestingly, *Df(2L)BSC6* mutant embryos also survived to late embryogenesis and showed identical defects in dorsal closure (Fig. 2D).

To demonstrate that the dorsal closure defects of *Sec61α*^{1} were due to the loss of *Sec61α*, we generated a genomic rescue construct consisting of the entire *Sec61α* gene and extending ~100 bp into the 5' UTR of the upstream gene *DLP* and ~350 bp into the 5' UTR of the downstream gene *CG9536* (Fig. 1A; note the genes are oriented in opposite directions). Four independent insertions of this construct rescued the embryonic lethality, and thus the dorsal closure defect of *Sec61α*^{1} mutant animals (Fig. 1E and Table 1). The rescue, however, was not complete with *Sec61α*^{1}. For example, although 95 (± 1)% of *Sec61α*^{1}*;P{Sec61α line CM15-1}* animals hatched as larvae, none of them eclosed and most died as pharate adults (Table 1). Rescue of *Sec61α*^{1}*/Sec61α*^{k04917} mutant animals with this *Sec61α* genomic construct was more complete, resulting in >70% viable adults (Table 1). Together these results suggest that either there is a very strong requirement for *Sec61α* in

late pupae that the rescue constructs cannot produce (but is enough in conjunction with *Sec61α*^{k04917}), or that the *Sec61α*^{1} chromosome possesses a second-site pupal lethal mutation.

Although *Sec61α*^{1} mutants showed a completely penetrant defect in dorsal closure, most other morphogenetic events occurring during mid embryogenesis continued to completion. Most notably, 100% of *Sec61α*^{1} mutant animals have normally involuted heads, even though dorsal closure has completely failed ($n > 500$ mutant embryos observed; Fig. 2B). We therefore assessed other embryonic morphogenetic events in *Sec61α*^{1} mutant embryos. To assess the morphogenesis of the peripheral nervous system we stained wild type and *Sec61α*^{1} mutant stage 14 embryos with an antibody that recognizes Neuroglian, and found that peripheral nervous system development was unaffected by lack of zygotic *Sec61α* expression (Supplemental Figs. 1A, B). Similarly we assessed the morphogenesis of the salivary glands by staining stage 14 wild type and *Sec61α*^{1} mutants with antibodies against Cor, and again found no differences (Supplemental Figs. 1C, D). We next used chitin binding probe, wheat germ agglutinin and antibodies against Uinflatable (a protein that localizes to the apical plasma membrane in tracheal cells; Zhang and Ward, 2009) to assess tracheal morphogenesis. Although the patterning of the tracheal system was unaffected in *Sec61α*^{1} mutant embryos, the diameter of the tracheal tubes was smaller (Supplemental Figs. 1E, F and data not shown). Tracheal morphogenesis requires the secretion of chitin into the lumen of the tracheae starting at stage 14. This chitin forms a cylinder in the center of the lumen that is required for proper radial expansion of the tracheae (Araujo et al., 2005; Devine et al., 2005; Tonning et al., 2005). Later in development, the expression and secretion putative chitin modifying enzymes encoded by *serpentine* and *vermiform* are required for tracheal length control (Luschnig et al., 2006; Wang et al., 2006). It appears that chitin secretion into the tracheal lumen is reduced in *Sec61α*^{1} mutant embryos resulting in the diametric defects, however since the tracheae are not convoluted nor show

other tracheal length defects, it is likely that the secretion of the putative chitin modifying enzymes occurred normally. One additional tracheal defect that was observed was a failure in the fusion of some tracheal metameres. ~ 50% of *Sec61α*^{1} mutant embryos had at least one discontinuity (n = 98, data not shown). Finally, just to exclude the possibility that *Sec61α* mutant embryos were dying about the time of dorsal closure, thus rendering these defects nonspecific, we generated time-lapse movies of late stage 17 *Sec61α*^{1} and *Sec61α*^{1}*/CyO, Dfd-EYFP* embryos and observed that the *Sec61α*^{1} mutant embryos were alive and moving through the end of embryogenesis (data not shown). Taken together these observations suggest that zygotic loss of *Sec61α*^{1} has very specific effects on the morphogenetic process of dorsal closure during mid embryogenesis.

Dorsal closure initiates but fails during the epithelial migration phase in *Sec61α* mutant embryos

In order to determine how zygotic loss of *Sec61α* might result in such specific defects in dorsal closure we first carefully examined the dorsal closure defects in *Sec61α*^{1} mutant embryos through a time course analysis. We collected wild type and mutant embryos at one hour intervals, aged them to 12-16 hours after egg laying, and stained them with antibodies against Cor to visualize the epidermis. Overall, *Sec61α* mutant embryos showed a one to two hour developmental delay and were going through dorsal closure when their heterozygous siblings had already completed the process. We therefore used gut and head morphology to accurately stage the animals. At the end of germ band retraction in mutant and wild type animals the cells of the lateral epidermis are polygonal in shape. During the initiation phase of dorsal closure in stage 13 wild type embryos the DME cells elongate in the dorsal-ventral axis (Fig. 3A), whereas the more ventral cells remain

polygonal. DME cells in stage 14 *Sec61α*^{1} mutant embryos also elongate in the dorsal-ventral axis, suggesting that initiation of dorsal closure had begun normally (Fig. 3C). Subsequently, during the epithelial migration phase of dorsal closure in wild type embryos, the more ventral lateral epidermal cells elongate dorsally as the epidermal sheets are coordinately pulled towards the dorsal midline (Figs. 3B, D). During this process the leading edge of the epidermis maintains an organized appearance showing a continuous curve along the anterior-posterior axis (Fig. 3B). In contrast, the leading edge of the epidermis appears disorganized and the lateral epidermal cells fail to fully elongate in stage 15 *Sec61α*^{1} mutant embryos (Fig. 3E). The DME cells eventually revert to a non elongated state (Figs. 3E, G). Finally, during the zippering phase of dorsal closure in wild type embryos (stage 15), the DME cells meet at the dorsal midline and fuse with the contralateral leading edge cells starting at the anterior and posterior ends and gradually suturing the epidermis towards the center (Figs. 3D, F). In *Sec61α*^{1} mutant embryos, although there is some zippering observed at the anterior and posterior ends of the epidermis, the majority of the DME cells never come in close apposition and therefore cannot fuse. Subsequently, either the amnioserosa tears away or is degraded (presumably through apoptosis), allowing the underlying brain and guts to protrude through the epidermal hole (Fig. 3G). Although we noted some variability in the extent to which *Sec61α*^{1} mutant embryos completed the epithelial migration phase, we never observed mutant embryos that were completely closed ($n > 500$ mutant embryos observed). Taken together, these observations suggest that initiation occurs normally in *Sec61α*^{1} mutant embryos, but that epithelial migration is severely affected.

Since the guts protrude from the dorsal surface in late stage 16 *Sec61α*^{1} mutant embryos (Fig. 3G), we wanted to address when the amnioserosa was breaking down in these animals. We therefore stained wild type and *Sec61α*^{1} mutant embryos with antibodies against phospho-tyrosine to visualize amnioserosal cells in addition to the epidermis. We found that the amnioserosa was

completely intact through stage 14 in the mutant embryos, just as in wild type (Figs. 3 H, I), but started to tear apart from the epidermis in stage 15 mutant embryos (Fig. 3 K).

One of the hallmarks of the specification of the DME cells is the execution of a Jun amino terminal kinase (JNK) signaling pathway. At the end of this signaling pathway, Jun and Fos induce the expression of *puckered* (*puc*), which encodes a phosphatase that negatively regulates the JNK pathway (Ring and Martinez Arias, 1993; Hou et al., 1997; Riesgo-Escovar and Hafen, 1997b). We therefore examined embryos produced by *Sec61α^{1}/Cyo, Dfd-EYFP ; puc^{E69}*/+ parents for the expression of *puc* (as determined by β-gal expression of the *puc* enhancer trap). In two independent experiments we examined 285 stage 14-16 embryos that we could unambiguously identify as either *Sec61α^{1}* or one of the two *EYFP* genotypes (*Sec61α^{1}/Cyo, Dfd-EYFP* or *Cyo, Dfd-EYFP/Cyo, Dfd-EYFP*). We could also distinguish each embryo as *puc^{E69}/ puc^{E69}*, *puc^{E69}*/+, or +/+. The same percentage of *Sec61α^{1}* embryos expressed *puc*, as did their non-mutant siblings (67% in both cases, with a Mendelian expectation of 75%). When we examined individual *Sec61α^{1};Puc^{E69}*/+ embryos we found that *puc* was clearly expressed in the DME cells. In fact, to the extent that we could tell by confocal microscopy, each DME cell expressed *puc* (Figs. 4A, B). Thus, loss of *Sec61α* did not appear to affect the JNK signaling pathway in the DME cells associated with the initiation of dorsal closure.

Zygotic loss of *Sec61α* attenuates Dpp signaling during dorsal closure

Another major consequence of JNK signaling in the DME cells is the expression and secretion of Dpp (Ring and Martinez Arias, 1993; Hou et al., 1997; Riesgo-Escovar and Hafen, 1997b). Dpp is a TGF-β/BMP ligand that binds to a receptor complex consisting of a Type-I receptor (encoded by

thick veins, *tkv*) and a type-II receptor (encoded by *punt*, *put*) in the epidermal cells and in the amnioserosa (Affolter et al., 1994; Nellen et al., 1994; Simin et al., 1998). All three of these proteins go through the secretory pathway and thus must enter the endoplasmic reticulum through Sec61α. Mutations in *tkv* and *put* show similar dorsal closure phenotypes including initial elongation of the DME cells and subsequent failure to maintain a uniform migration front at the leading edge with non elongated ventral epidermal cells (Riesgo-Escovar and Hafen, 1997a; Simin et al., 1998; Ricos et al., 1999). These defects in the organization of the DME cells and inability to drive the epidermal migration in *tkv* mutant embryos result in part from a loss of an actinomyosin cable in the DME cells (Zahedi et al., 2008). We therefore examined the expression of the myosin regulatory light chain (encoded by *spaghetti squash*; Karess et al., 1991) in the DME cells in $Sec61\alpha^{1}$ mutant embryos. Notably, Sqh was absent or very strongly reduced at the leading edge of the DME cells of stage 14 mutant embryos compared to wild type embryos (Figs. 5A, B). Sqh expression in the lateral epidermis was similar, however, between wild type and $Sec61\alpha^{1}$ mutant embryos, indicating that this is a specific loss of the myosin cable in the DME cells of $Sec61\alpha^{1}$ mutant embryos.

In order to more directly determine whether lack of zygotic *Sec61α* expression affected Dpp signaling, we examined the levels of phosphorylated Mothers Against Dpp (Mad) in wild type and $Sec61\alpha^{1}$ mutant embryos. The expression of phosphorylated Mad (pMad) has been extensively used as a readout of Dpp signaling at various stages of *Drosophila* development including during dorsal closure (e.g. Dorfman and Shilo, 2001; Fernandez et al., 2007). In early stage 14 wild type embryos, pMad is found at high levels in 4-5 rows of lateral epidermal cells ventral to the DME cells (Fig. 5C). In contrast, in four independent collections of $Sec61\alpha^{1}$ mutant embryos, we consistently observed strongly reduced or absent pMad staining in early stage 14 mutant embryos (Fig. 5D; n=51 early stage 14 $Sec61\alpha^{1}$ mutant embryos).

If a mutation in *Sec61α* affects dorsal closure through the expression of Dpp or one of its receptors, we reasoned that it should be possible to rescue that defect by specifically activating the Dpp signaling pathway during mid embryogenesis. We therefore used the UAS-GAL4 system (Brand and Perrimon, 1994) to express a constitutively activated form of the Tkv receptor (Nellen et al., 1996), tkv^{Q253D}, in the epidermis (using *e22c-* and *T80-Gal4;* Jacinto et al., 2000) or in the amnioserosa (*332.3-Gal4*; Harden et al., 2002) of $Sec61\alpha^{1}$ mutant embryos. Since the expression of tkv^{Q253D} did not rescue the cuticle defect of $Sec61\alpha^{1}$ mutant embryos (data not shown), we assessed the terminal phenotype of the mutant embryos by indirect immunofluorescence of 16-20 hour old mutant embryos stained with Cor. In control experiments we first determined that 100% (*n*=206) of 16-20 hour AEL $Sec61\alpha^{1}$ mutant embryos robustly stain with Cor antibodies, whereas only 1% (*n*=150) of $Sec61\alpha^{1}$/+ embryos stain well with Cor. We could thus identify the $Sec61\alpha^{1}$ mutant embryos in these experiments with near certainty. In addition we performed control experiments to examine the phenotypes of $Sec61\alpha^{1}$,*-Gal4/$Sec61\alpha^{1}$* (where * indicates *e22c* or *332.3*), and found that 100% of the embryos that stained with Cor at 16-20 hours AEL were completely dorsally open with the brains and guts extruded (Fig. 6A and data not shown). Experimentally we crossed *,*-Gal4, $Sec61\alpha^{1}$/CyO* flies to $Sec61\alpha^{1}$/+;UAS- tkv^{Q253D}/+ flies. Complete rescue of dorsal closure would result in 50% of the Cor staining embryos displaying a completely open dorsal surface and 50% showing a closed dorsal surface. Animals expressing *UAS-* tkv^{Q253D} using all three *Gal4* lines showed nearly completely penetrant rescue (Table 2). The degree of rescue was slightly variable, ranging from animals possessing a small dorsal hole, but with the brain and guts completely contained within the embryo (Fig. 6B), to animals with the lateral epidermal sheets completely apposed at the dorsal midline, but not necessarily fused (Fig. 6C). In general *e22c-Gal4* produced a stronger degree of rescue than *T80-Gal4* or *332.3-Gal4*. We conducted an identical set of experiments using *UAS-Dpp* instead of *UAS-* tkv^{Q253D}. We observed ~20% of the expected rescue

using *e22c-Gal4* to drive the expression of *Dpp*, with less penetrant rescue resulting from expression driven by *T80-Gal4* and *332.3-Gal4* (Table 2). The degree of rescue was similarly variable with the *UAS- tkv*^{Q253D}experiments (data not shown). Taken together, these results strongly indicate that zygotic loss of *Sec61α* results in specific defects in dorsal closure through a reduction in Dpp signaling during mid embryogenesis.

As a further test of the model that zygotic loss of *Sec61α* results in reduced Dpp signaling during mid embryogenesis, we analyzed midgut morphogenesis in *Sec61α*^{1} mutant embryos since Dpp is known to be required for this process (Immergluck et al., 1990; Panganiban et al., 1990). During midgut morphogenesis Dpp is secreted from the visceral mesoderm starting at stage 14 and is required in the underlying endoderm for the second midgut constriction. By stage 16 a four-chambered midgut is clearly apparent in wild type animals (Fig. 7A). Consistent with a reduction in Dpp signaling, we never observed a four-chambered midgut in stage 16 *Sec61α*^{1} mutant embryos (*n* > 100 mutant embryos). Although the guts were sometimes more extremely affected, the most obvious defect observed was a lack of the second midgut constriction (Fig. 7B). Since *Sec61α*^{1} mutant embryos eventually display extruded guts due to defective dorsal closure, and we observed a developmental delay in these animals, we wanted to be sure that we were not simply observing mutant animals prior to the formation of this constriction. We therefore examined the midgets in early stage 17 *Sec61α*^{1} mutant embryos that were expressing *tkv*^{Q253D} in the epidermis (using *e22c-Gal4*). Epidermal expression of Tkv^{Q253D} was sufficient to rescue dorsal closure to the point of preventing gut extrusion, but is not predicted to rescue any Dpp signaling defects in the mesoderm and underlying endoderm. We never observed a four-chambered midgut in these animals (Fig. 7C), consistent with the notion that Dpp signaling is particularly sensitive to the zygotic loss of *Sec61α* during mid embryogenesis.

DISCUSSION

Zygotic loss of *Sec61α* has a specific effect on dorsal closure

Sec61α encodes the major subunit of the translocon complex in the endoplasmic reticulum (reviewed in Johnson and van Waes, 1999). The translocon complex consists of three subunits: Sec61α, β, and γ, with the 10 transmembrane domain α subunit forming the major pore through the membrane. The truncated product of the *Sec61α*^{1} mutation, if expressed at all, would almost certainly produce a nonfunctional protein, and therefore prevent proteins from entering the ER and secretory pathway. The identical phenotypes observed in *Sec61α*^{1}, *Sec61α*^{1}*/Df(2L)BSC6* and even *Df(2L)BSC6* homozygous mutant embryos demonstrate that *Sec61α*^{1} is a nonfunctional, amorphic allele.

Sec61α is produced maternally and the maternal complement is likely partially functional at least through mid embryogenesis. The Berkeley *Drosophila* Genome Project gene expression pattern database shows that *Sec61α* is strongly expressed in stage 1-3 embryos (Tomancak et al., 2002). In addition, a *Sec61α:GFP* protein trap transgenic line is expressed in germline cysts (Snapp et al., 2004). Evidence that the maternal contribution still has function in mid embryogenesis includes direct and indirect measures of protein expression in *Sec61α*^{1} mutant embryos (that have a complete zygotic loss of *Sec61α*). For example, the transmembrane protein Neuroglian is expressed in *Sec61α*^{1} mutant embryos at levels indistinguishable to those of wild type embryos that were fixed and stained in parallel and imaged using the same parameters (Supplemental Fig. 1). We similarly observed only a slight reduction in the expression of the transmembrane proteins E-cadherin and α-integrin in mutant embryos as compared to wild type (data not shown). Since these proteins could

have been secreted hours previous, however, we wanted to assess a secreted protein that is not expressed until later in development. We can observe this indirectly through the function of Serpentine and Vermiform, two putative chitin deacetylases that are first synthesized in stage 12 embryos and subsequently secreted into the tracheal lumen at stage 14. These enzymes are required for tube length control in tracheae (Luschnig et al., 2006; Wang et al., 2006), and although there is reduced chitin secreted into the tracheae of *Sec61α*^{1} mutant embryos, tracheal length is not affected, suggesting that these enzymes were secreted and functioned properly (Supplemental Fig. 1). Taken together, these observations suggest that the maternal contribution of *Sec61α* still has some function (and perhaps fairly good function) at mid embryogenesis. By the end of embryogenesis, however, secretion appears to be more strongly affected as the mutant embryos fail to secrete chitin and thus display a naked cuticle phenotype.

At mid embryogenesis, the zygotic loss of *Sec61α* produces a highly specific and fully penetrant defect in dorsal closure. This phenotype is observed in *Sec61α*^{1}, *Sec61α*^{1}*/Df(2L)BSC6*, and even *Df(2L)BSC6* mutant animals. We were intrigued by the fact that although dorsal closure was completely disrupted in these embryos, head involution occurred normally, and therefore examined other developmental processes occurring roughly concurrently with dorsal closure that required secreted or transmembrane proteins for proper execution. For example, tracheal patterning and morphogenesis are dependent on several signaling pathways, most notably FGF signaling, which requires the transmembrane receptor Breathless in the tracheal cells to receive a secreted FGF signal encoded by *branchless* (reviewed in Affolter and Caussinus, 2008). Although the early events of patterning occur prior to dorsal closure, the formation and extension of the dorsal branch occurs during stages 12-15 of embryogenesis and require both the aforementioned FGF signaling pathway as well as Notch-Delta signaling to inhibit the cells ventral to the dorsal tip from becoming migratory. In addition, connecting the adjacent metamers to form a complete tracheal network

requires cell adhesion and specialized vesicle trafficking in the fusion cells that occurs during stages 14-16 (Jiang et al., 2007). Although one or two of metameres in about half of the embryos are not completely fused, the vast majority of these fusion events occurs normally, and thus it appears that tracheal morphogenesis is largely occurring normally in *Sec61α*^{1} mutant embryos (Supplemental Fig. 1 and data not shown). Similarly, the migration of the neurons and glia of the peripheral nervous system require guidance from secreted ligands and transmembrane receptors (reviewed in Cooper, 2002). We found that the peripheral neurons are correctly positioned in the *Sec61α*^{1} mutant embryos, again suggesting that the secretion of all these factors had occurred normally. Finally, the salivary gland is specified during stage 11 of embryogenesis, invaginates and executes a posterior migration over the visceral mesoderm during stage 14 (reviewed in Myat, 2005). This process requires the apposition of the salivary gland epithelium with the visceral mesoderm in a process requiring integrins. As shown in Supplemental Fig. 1, posterior migration of the salivary gland occurred normally in *Sec61α*^{1} mutant embryos. Thus, of all the morphogenetic events occurring simultaneously during mid embryogenesis, zygotic loss of *Sec61α* specifically perturbs dorsal closure.

It should be noted that zygotic loss of *Sec61β* does not show a similar defect in dorsal closure, but rather only shows defects in cuticle secretion late in embryogenesis (Valcarcel et al., 1999). Maternal loss of *Sec61β*, however, results in earlier embryonic lethality with defects in D-V patterning resulting from improper Gurken signaling (Valcarcel et al., 1999; Kelkar and Dobberstein, 2009). *Sec61β* encodes a peripheral component of the translocon complex that is not essential for protein translocation across the ER or for cell viability in yeast (Toikkanen et al., 1996; Leroux and Rokeach, 2008). Recent work in yeast has rather demonstrated a unique role for *Sec61β* in post-ER trafficking to the plasma membrane via the exocyst (Toikkanen et al., 2003). In support

of this, Kelkar and Dobberstein (2009) showed that Gurken is normally inserted into the ER in *Sec61β* germ line clones in *Drosophila*, but fails to traffic to the plasma membrane. Together these observations suggest that *Sec61β* does not have a strong effect on protein translocation into the ER, and thus it is not surprising that *Sec61β* does not show identical phenotypes to *Sec61α*.

Sec61α dorsal closure defects result from attenuated Dpp signaling

Dorsal closure is regulated by the complex interplay of several well-characterized signaling pathways including wingless, Notch, JNK and Dpp (Harden, 2002), most of which have components that are transmembrane or secreted (all of the JNK signaling proteins are cytoplasmic, although it has often been assumed that there is a membrane receptor necessary to initiate the cascade). The terminal phenotype of $Sec61\alpha^{1}$ and $Sec61\alpha^{1}$/*Df(2L)BSC6* mutant embryos is informative as the dorsal surface is completely exposed with extruded brain and guts, whereas the head involutes correctly. Mutations in JNK signaling component genes show similarly strong defects in dorsal closure, but additionally fail in head involution producing terminal phenotypes that are fully exposed from near the posterior pole through the head (for example Riesgo-Escovar and Hafen, 1997b). Thus any potential secreted upstream signals in the JNK signaling pathway appear to be unaffected by zygotic loss of *Sec61α*. Closer examination of the events of dorsal closure support this notion. The DME cells in $Sec61\alpha^{1}$ mutant embryos elongate in the D-V axis indicating that these cells had been correctly specified, a process requiring JNK signaling. Most telling, *puc* is expressed normally in the DME cells of mutant embryos (Fig. 4). Although observing the β-gal signal from the puc^{E69} enhancer trap line does not allow for a quantitative measure of the strength of

JNK signaling, it appeared that JNK signaling is active in every DME cell in *Sec61α*^{1} mutant embryos (Fig. 4B).

Our results strongly suggest that zygotic loss of *Sec61α* attenuates either the secretion of Dpp from the DME cells, or its reception in the epidermis and/or amnioserosa. Four pieces of evidence support this conclusion. First, the phenotypes associated with loss of *Sec61α* overlap those of mutations in the Dpp receptors *tkv* and *punt*. In all three mutations, the DME cells elongate in the D-V axis normally, whereas the lateral epidermal cells only partially elongate (Fig. 3; Riesgo-Escovar and Hafen, 1997a; Simin et al., 1998; Ricos et al., 1999). In addition, during the epithelial migration phase of dorsal closure the leading edge is irregular in both *tkv* and *Sec61α* mutant embryos (Fig. 3; Fernandez et al., 2007). Furthermore, the amnioserosa tears away from the epidermis in stage 15 *Sec61α*^{1} mutant embryos, just as it does in *tkv* mutant embryos (Fig. 3; Fernandez et al., 2007). Finally, the terminal phenotype observed in strong loss of function mutations in *Sec61α*, *tkv*, and *punt* is a large square dorsal hole accompanied by normal head involution (Fig. 2; Affolter et al., 1994; Nellen et al., 1994; Arora et al., 1995). The second piece of evidence in support of a loss of Dpp signaling in *Sec61α* mutant embryos is a strong reduction in the actinomyosin cable in the DME cells. Dpp regulates the expression of *zipper* (encoding nonmuscle myosin) in the DME cells (Arquier et al., 2001). We observed a strong and specific reduction in the levels of the myosin regulatory light chain (Sqh) in the DME cells, although we could clearly observe wild type levels of Sqh in other epidermal cells in the *Sec61α*^{1} mutant (Fig. 5). The third piece of evidence in support of reduced Dpp signaling is the elimination or strong reduction of pMad staining in the lateral epidermis in early stage 14 *Sec61α* mutant embryos (Fig. 5). The final and strongest piece of evidence implicating loss of Dpp signaling in *Sec61α*^{1} mutant embryos was the highly penetrant and very strong rescue of dorsal closure by *tkv*^{Q253D} (Table 2 and

Fig. 6), and the less penetrant, yet equally strong, rescue of *Sec61α*^{1} mutant embryos by epidermal expression of *Dpp* (Table 2).

It is noteworthy that although the penetrance of the rescue was similar if *tkv*^{Q253D} was expressed in the epidermis (*e22c-Gal4* or *T80-Gal4*) or the amnioserosa (*332.3-Gal4*), the overall strength of the rescue (degree of closure) was more pronounced with the epidermal expression. These results are consistent with the observations of Fernandez et al. (2007) that the expression of *tkv*^{Q253D} in the epidermis gave stronger rescue of the dorsal closure defects in strong loss of function *tkv* mutants (in terms of penetrance in this case) than expression in the amnioserosa. Our results further support their conclusion that Dpp signaling is required in both the epidermis and amnioserosa for normal dorsal closure. Finally, it is not surprising that the rescue of *Sec61α*^{1} by *tkv*^{Q253D} was not complete since the Tkv^{Q253D} protein would have had to go through the secretory pathway, and thus may not have been expressed at comparable levels to the experiments aimed at rescuing a *tkv* mutation (Fernandez et al., 2007).

Our results also suggest that Dpp signaling is attenuated, but likely not eliminated by zygotic loss of *Sec61α*. This notion is supported by the observation that although the phenotypes are similar between *Sec61α*^{1} and *tkv* mutants, there are minor differences. Specifically, in *tkv* mutant embryos, the DME cells bunch together at segmental boundaries (Ricos et al., 1999), and although we observed this phenotype in *Sec61α*^{1} embryos, the penetrance was substantially reduced (data not shown). In addition, although we found strong reductions in the actinomyosin cable in the leading edge of *Sec61α*^{1} mutant embryos, we still could observe a faint, often discontinuous, cable linking DME cells (Fig. 5). We also occasionally observed pMad staining in the lateral epidermis of *Sec61α*^{1} mutant embryos, although it was always clearly attenuated compared to wild type embryos (Fig. 5).

Taken together these results suggest a model in which zygotic loss of *Sec61α* gradually reduces traffic through the secretory pathway as the maternal stores are turned over, eventually resulting in a situation in which the expression of a dose-sensitive secreted protein falls below a critical threshold necessary to support dorsal closure. Our results indicate that the protein in question functions in the Dpp signaling pathway, and thus is most likely Dpp or one of its receptors. The observation of defective midgut constrictions in *Sec61α* mutant animals (Fig. 7) further supports the notion that Dpp signaling is specifically sensitive to loss of *Sec61α* at this stage of development, since Dpp signaling during mid embryogenesis is necessary for the formation of the second midgut constriction (Immergluck et al., 1990; Panganiban et al., 1990). Our experiments, however, could not definitively distinguish whether the dose-sensitive factor was Dpp itself or one of its receptors, but the tkv^{Q253D} rescue experiments argue that it has to be at the level of one of the receptors or upstream in the pathway. In addition, the rescue of dorsal closure in *Sec61α* embryos by epidermal expression of Dpp indicates that there is not a complete absence of Tkv or Put at the plasma membrane. We suggest that Dpp is the most likely candidate, as *dpp* is one of the few haploinsufficient genes encoded by the *Drosophila* genome (Spencer et al., 1982). *dpp* expression must be finely controlled in early embryogenesis due to its role as a morphogen for initial D-V patterning of the embryo (reviewed in O'Connor et al., 2006). Perhaps the dose-sensitivity of Dpp or its receptors during dorsal closure is a consequence of this earlier requirement to maintain precise levels of Dpp, although it is also possible that Dpp signaling during dorsal closure requires similar levels of tight control to precisely coordinate the cellular behaviors of at least two distinct tissues, the lateral epidermis and the amnioserosa.

EXPERIMENTAL PROCEDURES

Drosophila Strains

Sec61α^{1} is an EMS induced mutation on the *E(br)165* chromosome reported in Ward et al. (2003). *P{lacW}Sec61α*^{k04917}, *Df(2L)BSC6*, *332.3-Gal4*, *e22c-Gal4*, *T80-Gal4*, *UAS-Dpp, puc*^{E69}, and *w*^{1118} were obtained from the Bloomington *Drosophila* Stock Center (Bloomington, IN). *UAS-Tkv*^{Q253D} (Nellen et al., 1996) was obtained from Matt Gibson (Stowers Institute). *w*^{1118} was used as the wild type strain for all the experiments reported here. All *Drosophila* stocks were maintained on media consisting of corn meal, sugar, yeast, and agar in incubators maintained at a constant temperature of 21°C or in a room that typically fluctuated between 21°C and 22.5°C. Genetic experiments were conducted in incubators controlled at a constant temperature of 25ºC.

Molecular Analysis of *Sec61α*^{1}

Complementation analyses confirmed a lethal mutation in the region uncovered by *Df(2L)BSC6* (breakpoints 26D3;26F7) that also failed to complement the P-element allele *P{lacW}Sec61α*^{k04917}. Sequencing of genomic DNA isolated from homozygous mutant late embryos (by the DNA Facility of the Iowa State University Office of Biotechnology in Ames, IA) confirmed that the chromosome had a mutation in *Sec61α.* Both DNA strands were sequenced to confirm this result.

To generate a *Sec61α* genomic rescue construct, we PCR amplified genomic DNA isolated from *w*^{1118} embryos using the following primers: 5'-TCGGCACTAGCACTGAATACT-3' and 5'-ATAGCAGGTAGCCGAACGTG-3'. This generated a 4.4 kb genomic fragment containing all of *Sec61α* and extending ~100 bp into the upstream gene *DLP* and ~350 bp into the downstream gene *CG9536* (Note that these genes are oriented in opposite directions, and thus the genomic rescue construct only extends into the 5' UTR of each gene). We blunt-end ligated this fragment into a

StuI-cut pCasper 4 vector (Thummel et al., 1988). We checked orientation by restriction digest and sequenced the *Sec61α* portion of the plasmid (Iowa State University DNA Facility). The plasmid was injected into w^{1118} embryos at the Duke University Model System Genomics facility (Duke University, Durham, NC). We crossed four independent third chromosome inserts into our $Sec61\alpha^{1}$ stock, and all four rescued the embryonic lethality of $Sec61\alpha^{1}$.

Lethal Phase and Phenotypic Analyses

$Sec61\alpha^{1}$, $P\{lacW\}Sec61\alpha^{k04917}$ and *Df(2L)BSC6* were balanced with *CyO, P{w+, Dfd-EYFP}* (Le et al., 2006) in order that mutant embryos and larvae could be unambiguously identified by the absence of YFP. In order to identify mutant animals at earlier stages of development, we also balanced $Sec61\alpha^{1}$ with *CyO, P{ftz/lacB}*. Embryos were collected for four hours at 25ºC, aged for twelve hours and then selected based upon the absence of YFP. Embryonic lethality was determined as the percentage of unhatched embryos 48 hours after selecting non-YFP-expressing mutant embryos produced through a four-hour egg collection. Larval lethality was determined as the percentage of non-pupariating mutant larvae seven days after selecting newly hatched mutant larvae. Pupal lethality was determined as the percentage of non-eclosing mutant pupae ~seven days after pupariating. All experiments were performed in triplicate and means with standard deviations were determined. Non-hatched embryos were dechorionated in 6% sodium hypochloride, mounted on microscope slides in Hoyer's medium and subsequently examined for cuticular phenotypes on a Nikon Eclipse 80*i* compound microscope. All cuticular phenotypes were documented on a Nikon Eclipse 80*i* compound microscope equipped with a Photometrics CoolSNAP *ES* high performance digital CCD camera. Photomicrographs were cropped and adjusted for brightness and contrast with Adobe Photoshop (version CS3, San Jose, CA), and figures were compiled in Adobe Illustrator (version CS3, San Jose, CA).

Time-lapse movies were generated by mounting stage 17 *Sec61α^{1}/CyO, P{w^{+}, Dfd-EYFP}* and *Sec61α^{1}* mutant embryos on apple juice plates. We first collected a fluorescence image to distinguish the mutant and heterozygous embryos by YFP expression, and then automatically collected brightfield images every minute for 140 minutes using MetaMorph (Molecular Devices, Sunnyvale, CA) software on a Nikon Eclipse 80*i* compound microscope equipped with a Photometrics CoolSNAP *ES* high performance digital CCD camera using a 4X Nikon Plan Apo lens.

Antibody Production and Immunostaining

A Spaghetti squash (Sqh)-GST fusion protein was generated by blunt-end ligating nucleotides 217 to 811 of GenBank nucleotide sequence AY122159 (generated by PCR and verified by sequence analysis) into a PGEX2TK vector (GE Healthcare Bio-Sciences AB, Uppsala, Sweden) digested with SmaI. This fragment represents the entire coding sequence of Sqh. The protein was overexpressed in *E. Coli* BL21 (DE3) cells, and purified on glutathione sepharose 4 fast flow (GE Healthcare) according to standard procedures (Rebay and Fehon, 2000). Purified protein was used for antibody generation in mice at the Pocono Rabbit Farm and Laboratory Inc. (PRF&L, Canadensis, PA).

Embryos were fixed and processed for antibody staining as described (Fehon et al., 1991). Embryonic staging was determined by gut morphology. The following primary antibodies were used at the given dilutions: mouse anti-Neuroglian 1:100 (clone BP104 from the Developmental Studies Hybridoma Bank at the University of Iowa, Iowa City, IA), mouse anti-β-galactosidase 1:100 (clone 40-1a, DSHB), mouse anti-Fasciclin III 1:100 (clone 7G10, DSHB), mouse anti-phosphoMAD 1:250 (from P. ten Dijke), mouse anti-Sqh 1:1000, guinea pig anti-Uninflatable 1:20 (Zhang and Ward, 2009), rabbit anti-GFP 1:250 (Clontech, Mountain View, CA), mouse anti-

Coracle 1:400 and guinea pig anti-Coracle 1:10,000 (gifts from Richard Fehon, University of Chicago; Fehon et al., 1994), and FITC conjugated monoclonal anti-phosphotyrosine (Sigma, St. Louis, MO) 1:50. Secondary antibodies were obtained from Jackson ImmunoResearch Laboratories (West Grove, PA) and used at 1:800. Alexa Fluor 555 conjugated wheat germ agglutinin (WGA) was used at a concentration of 5μg/ml (Invitrogen, Carlsbad, CA). Rhodamine conjugated Chitin Binding Probe (CBP) was used at 1:500 according to the manufacturers recommendation (New England Biolabs Inc., Beverly, MA). Confocal images were acquired on a Zeiss LSM510 Meta Laser Scanning Confocal Microscope (Carl Zeiss Inc, Thornwood, NY). Photomicrographs were cropped and adjusted for brightness and contrast with Adobe Photoshop, and figures were compiled in Adobe Illustrator. The photomicrographs used to compile Fig. 4 were additionally modified with an unsharp mask filter (50%, 3 pixel radius, 5 level threshold) in Adobe Photoshop.

Dpp and tkv^{Q253D} Rescue Experiments

We first individually recombined *T80-Gal4*, *e22c-Gal4*, and *332.2-Gal4* onto *Sec61α^{1}* chromosomes, and balanced then over *CyO, P{w^{+}, Dfd-EYFP}*, creating *-Gal4, *Sec61α^{1}/CyO, P{w^{+}, Dfd-EYFP}*. We then crossed *UAS-tkv^{Q253D}* and *UAS-Dpp* into *Sec61α^{1}/CyO, P{w^{+}, Dfd-EYFP}*, creating *Sec61α^{1}/+; UAS-tkv^{Q253D}/+* and *Sec61α^{1}/+; UAS-Dpp/+*. Finally we crossed these *Gal4* and *UAS-tkv^{Q253D}* lines together and collected embryos from a 4 hour collection. We aged the embryos for 16 hours such that all the embryos would be 16-20 hours after egg laying. At this point all *Sec61α^{1}/+* embryos would have completed dorsal closure and secreted cuticle that would prevent the embryos from being stained with antibodies. We fixed and stained the embryos as described above, and examined all stained embryos for dorsal open phenotypes. We considered an embryo to have been rescued if the dorsal hole was small and the brain and guts were completely confined to the interior of the animal. Since only half of the *Sec61α^{1}* mutant embryos would contain

either *UAS-tkv*^{Q253D}/+ or *UAS-Dpp*/+, the % rescue reported in Table 2 would have a theoretical maximum value of 50%. The experiment was done in triplicate and mean with standard deviations were calculated.

ACKNOWLEDGMENTS

We thank Elspeth Pearce for help with construction of the *Sec61α* rescue construct, and members of the lab and anonymous reviewers for helpful comments about the manuscript. We thank Greg Beitel, Matt Gibson, and the Bloomington *Drosophila* Stock Center for fly stocks used in this study. We thank Richard Fehon, Rebecca Hays and the developmental studies hybridoma bank for the antibodies used in this study. The project was supported by NIH Grant Number P20 RR15563 and NIH Grant Number R01HD047570 from the National Center for Research Resources.

REFERENCES

Affolter M, Caussinus E. 2008. Tracheal branching morphogenesis in Drosophila: new insights into cell behaviour and organ architecture. Development 135:2055-2064.

Affolter M, Nellen D, Nussbaumer U, Basler K. 1994. Multiple requirements for the receptor serine/threonine kinase thick veins reveal novel functions of TGF beta homologs during Drosophila embryogenesis. Development 120:3105-3117.

Araujo SJ, Aslam H, Tear G, Casanova J. 2005. mummy/cystic encodes an enzyme required for chitin and glycan synthesis, involved in trachea, embryonic cuticle and CNS development--analysis of its role in Drosophila tracheal morphogenesis. Dev. Biol. 288:179-193.

Arora K, Dai H, Kazuko SG, Jamal J, O'Connor MB, Letsou A, Warrior R. 1995. The Drosophila schnurri gene acts in the Dpp/TGF beta signaling pathway and encodes a transcription factor homologous to the human MBP family. Cell 81:781-790.

Arquier N, Perrin L, Manfruelli P, Semeriva M. 2001. The Drosophila tumor suppressor gene lethal(2)giant larvae is required for the emission of the Decapentaplegic signal. Development 128:2209-2220.

Baumgartner S, Littleton JT, Broadie K, Bhat MA, Harbecke R, Lengyel JA, Chiquet-Ehrismann R, Prokop A, Bellen HJ. 1996. A Drosophila neurexin is required for septate junction and blood-nerve barrier formation and function. Cell 87:1059-1068.

Bloor JW, Kiehart DP. 2002. Drosophila RhoA regulates the cytoskeleton and cell-cell adhesion in the developing epidermis. Development 129:3173-3183.

Cooper HM. 2002. Axon guidance receptors direct growth cone pathfinding: rivalry at the leading edge. Int. J. Dev. Biol. 46:621-631.

Devine WP, Lubarsky B, Shaw K, Luschnig S, Messina L, Krasnow MA. 2005. Requirement for chitin biosynthesis in epithelial tube morphogenesis. Proc. Natl. Acad. Sci. U S A 102:17014-17019.

Dorfman R, Shilo BZ. 2001. Biphasic activation of the BMP pathway patterns the Drosophila embryonic dorsal region. Development 128:965-972.

Fehon RG, Dawson IA, Artavanis-Tsakonas S. 1994. A Drosophila homologue of membrane-skeleton protein 4.1 is associated with septate junctions and is encoded by the coracle gene. Development 120:545-557.

Fehon RG, Johansen K, Rebay I, Artavanis-Tsakonas S. 1991. Complex cellular and subcellular regulation of notch expression during embryonic and imaginal development of Drosophila: implications for notch function. J. Cell Biol. 113:657-669.

Fernandez BG, Arias AM, Jacinto A. 2007. Dpp signalling orchestrates dorsal closure by regulating cell shape changes both in the amnioserosa and in the epidermis. Mech. Dev. 124:884-897.

Franke JD, Montague RA, Kiehart DP. 2005. Nonmuscle myosin II generates forces that transmit tension and drive contraction in multiple tissues during dorsal closure. Curr. Biol. 15:2208-2221.

Glise B, Noselli S. 1997. Coupling of Jun amino-terminal kinase and Decapentaplegic signaling pathways in Drosophila morphogenesis. Genes Dev. 11:1738-1747.

Harden N. 2002. Signaling pathways directing the movement and fusion of epithelial sheets: lessons from dorsal closure in Drosophila. Differentiation 70:181-203.

Harden N, Ricos M, Yee K, Sanny J, Langmann C, Yu H, Chia W, Lim L. 2002. Drac1 and Crumbs participate in amnioserosa morphogenesis during dorsal closure in Drosophila. J. Cell Sci. 115:2119-2129.

Hou XS, Goldstein ES, Perrimon N. 1997. Drosophila Jun relays the Jun amino-terminal kinase signal transduction pathway to the Decapentaplegic signal transduction pathway in regulating epithelial cell sheet movement. Genes Dev. 11:1728-1737.

Hutson MS, Tokutake Y, Chang MS, Bloor JW, Venakides S, Kiehart DP, Edwards GS. 2003. Forces for morphogenesis investigated with laser microsurgery and quantitative modeling. Science 300:145-149.

Immergluck K, Lawrence PA, Bienz M. 1990. Induction across germ layers in Drosophila mediated by a genetic cascade. Cell 62:261-268.

Jacinto A, Wood W, Balayo T, Turmaine M, Martinez-Arias A, Martin P. 2000. Dynamic actin-based epithelial adhesion and cell matching during Drosophila dorsal closure. Curr. Biol. 10:1420-1426.

Jacinto A, Woolner S, Martin P. 2002. Dynamic analysis of dorsal closure in Drosophila: from genetics to cell biology. Dev. Cell 3:9-19.

Jasper H, Benes V, Schwager C, Sauer S, Clauder-Munster S, Ansorge W, Bohmann D. 2001. The genomic response of the Drosophila embryo to JNK signaling. Dev. Cell 1:579-586.

Jiang L, Rogers SL, Crews ST. 2007. The Drosophila Dead end Arf-like3 GTPase controls vesicle trafficking during tracheal fusion cell morphogenesis. Dev. Biol. 311:487-499.

Johnson AE, van Waes MA. 1999. The translocon: a dynamic gateway at the ER membrane. Annu. Rev. Cell Dev. Biol. 15:799-842.

Karess RE, Chang XJ, Edwards KA, Kulkarni S, Aguilera I, Kiehart DP. 1991. The regulatory light chain of nonmuscle myosin is encoded by spaghetti-squash, a gene required for cytokinesis in Drosophila. Cell 65:1177-1189.

Kelkar A, Dobberstein B. 2009. Sec61beta, a subunit of the Sec61 protein translocation channel at the endoplasmic reticulum, is involved in the transport of Gurken to the plasma membrane. BMC Cell Biol. 10:11.

Kiehart DP, Galbraith CG, Edwards KA, Rickoll WL, Montague RA. 2000. Multiple forces contribute to cell sheet morphogenesis for dorsal closure in Drosophila. J. Cell Biol. 149:471-490.

Le T, Liang Z, Patel H, Yu MH, Sivasubramaniam G, Slovitt M, Tanentzapf G, Mohanty N, Paul SM, Wu VM, Beitel GJ. 2006. A new family of Drosophila balancer chromosomes with a w- dfd-GMR yellow fluorescent protein marker. Genetics 174:2255-2257.

Leptin M, Bogaert T, Lehmann R, Wilcox M. 1989. The function of PS integrins during Drosophila embryogenesis. Cell 56:401-408.

Leroux A, Rokeach LA. 2008. Inter-species complementation of the translocon beta subunit requires only its transmembrane domain. PLoS One 3:e3880.

Luschnig S, Batz T, Armbruster K, Krasnow MA. 2006. serpentine and vermiform encode matrix proteins with chitin binding and deacetylation domains that limit tracheal tube length in Drosophila. Curr. Biol. 16:186-194.

Manfruelli P, Arquier N, Hanratty WP, Semeriva M. 1996. The tumor suppressor gene, lethal(2)giant larvae (1(2)g1), is required for cell shape change of epithelial cells during Drosophila development. Development 122:2283-2294.

Miyamoto H, Nihonmatsu I, Kondo S, Ueda R, Togashi S, Hirata K, Ikegami Y, Yamamoto D. 1995. canoe encodes a novel protein containing a GLGF/DHR motif and functions with Notch and scabrous in common developmental pathways in Drosophila. Genes Dev. 9:612-625.

Mizuno T, Tsutsui K, Nishida Y. 2002. Drosophila myosin phosphatase and its role in dorsal closure. Development 129:1215-1223.

Myat MM. 2005. Making tubes in the Drosophila embryo. Dev. Dyn. 232:617-632.

Narasimha M, Brown NH. 2004. Novel functions for integrins in epithelial morphogenesis. Curr. Biol. 14:381-385.

Nellen D, Affolter M, Basler K. 1994. Receptor serine/threonine kinases implicated in the control of Drosophila body pattern by decapentaplegic. Cell 78:225-237.

Nellen D, Burke R, Struhl G, Basler K. 1996. Direct and long-range action of a DPP morphogen gradient. Cell 85:357-368.

O'Connor MB, Umulis D, Othmer HG, Blair SS. 2006. Shaping BMP morphogen gradients in the Drosophila embryo and pupal wing. Development 133:183-193.

Panganiban GE, Reuter R, Scott MP, Hoffmann FM. 1990. A Drosophila growth factor homolog, decapentaplegic, regulates homeotic gene expression within and across germ layers during midgut morphogenesis. Development 110:1041-1050.

Peifer M, Wieschaus E. 1990. The segment polarity gene armadillo encodes a functionally modular protein that is the Drosophila homolog of human plakoglobin. Cell 63:1167-1176.

Perrimon N. 1988. The maternal effect of lethal(1)discs-large-1: a recessive oncogene of Drosophila melanogaster. Dev. Biol. 127:392-407.

Rebay I, Fehon RG. 2000. Generating antibodies against Drosophila proteins. In: Sullivan W, Ashburner M, Hawley RS, editors. Drosophila Protocols. Cold Spring Harbor, New York: Cold Spring Harbor Laboratory Press. pp 389-411.

Reed BH, Wilk R, Lipshitz HD. 2001. Downregulation of Jun kinase signaling in the amnioserosa is essential for dorsal closure of the Drosophila embryo. Curr. Biol. 11:1098-1108.

Reed BH, Wilk R, Schock F, Lipshitz HD. 2004. Integrin-dependent apposition of Drosophila extraembryonic membranes promotes morphogenesis and prevents anoikis. Curr. Biol. 14:372-380.

Ricos MG, Harden N, Sem KP, Lim L, Chia W. 1999. Dcdc42 acts in TGF-beta signaling during Drosophila morphogenesis: distinct roles for the Drac1/JNK and Dcdc42/TGF-beta cascades in cytoskeletal regulation. J. Cell Sci. 112 (Pt 8):1225-1235.

Riesgo-Escovar JR, Hafen E. 1997a. Common and distinct roles of DFos and DJun during Drosophila development. Science 278:669-672.

Riesgo-Escovar JR, Hafen E. 1997b. Drosophila Jun kinase regulates expression of decapentaplegic via the ETS-domain protein Aop and the AP-1 transcription factor DJun during dorsal closure. Genes Dev. 11:1717-1727.

Ring JM, Martinez Arias A. 1993. puckered, a gene involved in position-specific cell differentiation in the dorsal epidermis of the Drosophila larva. Development Suppl.:251-259.

Simin K, Bates EA, Horner MA, Letsou A. 1998. Genetic analysis of punt, a type II Dpp receptor that functions throughout the Drosophila melanogaster life cycle. Genetics 148:801-813.

Snapp EL, Iida T, Frescas D, Lippincott-Schwartz J, Lilly MA. 2004. The fusome mediates intercellular endoplasmic reticulum connectivity in Drosophila ovarian cysts. Mol. Biol. Cell 15:4512-4521.

Spencer FA, Hoffmann FM, Gelbart WM. 1982. Decapentaplegic: a gene complex affecting morphogenesis in Drosophila melanogaster. Cell 28:451-461.

Stark KA, Yee GH, Roote CE, Williams EL, Zusman S, Hynes RO. 1997. A novel alpha integrin subunit associates with betaPS and functions in tissue morphogenesis and movement during Drosophila development. Development 124:4583-4594.

Thummel CS, Boulet AM, Lipshitz HD. 1988. Vectors for Drosophila P-element-mediated transformation and tissue culture transfection. Gene 74:445-456.

Toikkanen J, Gatti E, Takei K, Saloheimo M, Olkkonen VM, Soderlund H, De Camilli P, Keranen S. 1996. Yeast protein translocation complex: isolation of two genes SEB1 and SEB2 encoding proteins homologous to the Sec61 beta subunit. Yeast 12:425-438.

Toikkanen JH, Miller KJ, Soderlund H, Jantti J, Keranen S. 2003. The beta subunit of the Sec61p endoplasmic reticulum translocon interacts with the exocyst complex in Saccharomyces cerevisiae. J. Biol. Chem. 278:20946-20953.

Tomancak P, Beaton A, Weiszmann R, Kwan E, Shu S, Lewis SE, Richards S, Ashburner M, Hartenstein V, Celniker SE, Rubin GM. 2002. Systematic determination of patterns of gene expression during Drosophila embryogenesis. Genome Biol. 3:RESEARCH0088.

Tonning A, Hemphala J, Tang E, Nannmark U, Samakovlis C, Uv A. 2005. A transient luminal chitinous matrix is required to model epithelial tube diameter in the Drosophila trachea. Dev. Cell 9:423-430.

Valcarcel R, Weber U, Jackson DB, Benes V, Ansorge W, Bohmann D, Mlodzik M. 1999. Sec61beta, a subunit of the protein translocation channel, is required during Drosophila development. J. Cell Sci. 112:4389-4396.

Wang S, Jayaram SA, Hemphala J, Senti KA, Tsarouhas V, Jin H, Samakovlis C. 2006. Septate-junction-dependent luminal deposition of chitin deacetylases restricts tube elongation in the Drosophila trachea. Curr. Biol. 16:180-185.

Ward RE, Evans J, Thummel CS. 2003. Genetic modifier screens in Drosophila demonstrate a role for Rho1 signaling in ecdysone-triggered imaginal disc morphogenesis. Genetics 165:1397-1415.

Young PE, Richman AM, Ketchum AS, Kiehart DP. 1993. Morphogenesis in Drosophila requires nonmuscle myosin heavy chain function. Genes Dev. 7:29-41.

Zahedi B, Shen W, Xu X, Chen X, Mahey M, Harden N. 2008. Leading edge-secreted Dpp cooperates with ACK-dependent signaling from the amnioserosa to regulate myosin levels during dorsal closure. Dev. Dyn. 237:2936-2946.

Zhang L, Ward RE. 2009. uninflatable encodes a novel ectodermal apical surface protein required for tracheal inflation in Drosophila. Dev. Biol. 336:201-212.

FIGURE LEGENDS

Fig. 1. Molecular organization of the *Sec61α* locus, and embryonic cuticle defects associated with zygotic loss of function alleles of *Sec61α*. (A) Schematic diagrams of the genomic locus (top), transcript (middle), and protein of *Sec61α*. The centromere is to the right of this genomic fragment. The transcript is drawn to scale with the genomic diagram, with exons depicted as rectangles and coding regions filled with black. Introns are depicted as bent lines below the exons. Black bars in the protein schematic represent the location of the ten transmembrane domains. The genomic region used as a rescue construct is indicated by the bracketed line. *P{lacW} Sec61α*^{k04917} in inserted into the second intron as shown. The location of the *Sec61α*^{1} mutation is indicated by an arrow in the transcript and an asterisk in the protein. The nucleotide and protein sequences of the *Sec61α*^{1} mutation are shown below the protein. Nucleotide sequence number is based on GenBank sequence **AY069569**. (B-E) Brightfield photomicrographs of cuticle preparations from wild type and *Sec61α* mutant animals. (B) A *w*^{1118} late stage 17 embryo showing normal cuticular features including ventral denticle belts (arrowheads) and head skeleton (arrow). (C) A *Sec61α*^{1} mutant embryo showing no cuticular features. (D) A *Sec61α*^{1}*/Df(2L)BSC6* mutant embryo also showing no cuticle. (E) A *Sec61α*^{1} late stage 17 mutant embryo containing two copies of the *Sec61α* genomic rescue fragment inserted on the third chromosome shows normal cuticular features. All embryos are depicted with anterior to the left and the dorsal surface facing up. The embryos in (B) and (E) were taken prior to hatching, but would have hatched given the chance.

Fig. 2. *Sec61α* mutant animals show defects in dorsal closure. (A-D) Confocal optical sections of (A) *w*^{1118} stage 16 embryo, (B) *Sec61α*^{1} late stage 17 embryo, (C) *Sec61α*^{1}*/Df(2L)BSC6* late

stage 17 embryo, and (D) *Df(2L)BSC6* late stage 17 embryo all stained with antibodies against Coracle to visualize cell outlines in the epidermis. Anterior is to the left and dorsal is up in all cases. Note that in all the mutant animals there is no epidermal cells covering the dorsal surface, and the brain (arrows) and guts (arrowheads) are extruded from the dorsal hole. Note that although dorsal closure has failed, head involution has occurred (asterisk in B indicates the dorsal anterior region of the epidermis after head involution had occurred). (Scale bar: 20μm).

Fig. 3. *Sec61α* mutant animals initiate dorsal closure but fail during the epithelial migration phase. (A-G) Confocal optical sections of w^{1118} (A, B, D, F) and $Sec61\alpha^{1}$ (C, E, G) embryos stained with antibodies against Coracle (Cor) to visualize epidermal cells during dorsal closure. Anterior is to the left in all cases and lateral or dorsal views are shown. A', B' etc show higher magnification views of the DME cells and lateral epidermis of the embryos shown in A, B etc. (A, A') Stage 13 wild type embryo showing the initiation of dorsal closure. Note that the DME cells are elongated in the dorsal-ventral (D-V) axis (arrowheads in A'), whereas the lateral epidermal cells remain polygonal. (B, B') Stage 14 wild type embryo showing D-V elongation of both the DME cells and the lateral epidermis. Note also the uniform curvature of the leading edge of the epithelium (arrowheads in B). (C, C') Stage 14 $Sec61\alpha^{1}$ mutant embryo showing elongated DME cells and mostly elongated lateral epidermal cells. (D, D') Stage 15 wild type embryo near the completion of dorsal closure. The DME cells are still elongated and the contraleteral DME cells are zippering together starting at the anterior and posterior ends. (E, E') Stage 15 $Sec61\alpha^{1}$ mutant embryo. The DME cells and lateral epidermis are not strongly elongated in the D-V axis, and the leading edge does not present a uniformly curved appearance. The amnioserosa is still intact in this embryo as the brain and guts have not broken through the dorsal surface. (F, F') Stage 16 wild type embryo after the completion of dorsal closure. (G, G') Stage 16 $Sec61\alpha^{1}$ mutant embryo after dorsal closure has

failed. In this case the all of the epidermal cells are polygonal, the leading edge of the epidermis is irregular and the amnioserosa has clearly degraded or been torn away as the hindgut is protruding through the dorsal surface (arrow). Note also that head involution has occurred normally (arrowheads). (H-K) confocal optical sections of w^{1118} (H, J) and $Sec61\alpha^{1}$ (I, K) embryos stained with antibodies against Phospho-tyrosine (PY) to visualize the amnioserosa and epidermis during dorsal closure. The amnioserosa is intact in w^{1118} stage 14 (H) and stage 15 (J) embryos, as well as in the stage 14 $Sec61\alpha^{1}$ mutant embryo (I), but has torn away from the epidermis of the stage 15 $Sec61\alpha^{1}$ mutant embryo (arrows in K). (scale bars: 20μm).

Fig. 4. JNK signaling occurs normally in the DME cells of Sec61α mutant embryos. Confocal optical sections of a $Sec61\alpha^{1}$/CyO, P{Dfd-YFP};puc^{E69}/+ stage 14 embryo (A) and a $Sec61\alpha^{1}$;puc^{E69}/+ stage 14 embryo stained with antibodies against Cor (in green) to outline epidermal cells and against β-Gal to recognize puc^{E69} expression (red) in the DME cells. Note that each DME cell expresses *puc* in both mutant and heterozygous embryos. Anterior is to the left and dorsal is up in all these images.

Fig. 5. The actinomyosin cable is strongly reduced or eliminated in the DME cells of Sec61α mutant embryos, and Dpp signaling is attenuated. (A, B) Confocal optical sections of stage 14 w^{1118} (A) and $Sec61\alpha^{1}$ (B) mutant embryos stained for antibodies against Spaghetti squash (Sqh, red) and Coracle (Cor, green). A' and B' show the Sqh channel alone. Cor staining outlines the epidermal cells and clearly shows the interface between the DME cells and the amnioserosa. Note the thick cable of Sqh running through the leading edge of the wild type DME cells that is nearly absent in the $Sec61\alpha^{1}$ mutant embryo (arrowheads). (C, D) Confocal optical sections of stage 14

w^{1118} (C) and $Sec61\alpha^{1}$ (D) mutant embryos stained for antibodies against phosphorylated Mad (pMad, red) and Coracle (Cor, green). C' and D' show the pMad channel alone. In the w^{1118} embryo, pMad is strongly expressed in the nuclei of lateral epidermal cells in a band that extends 4-5 cells ventral to the DME cells. In the $Sec61\alpha^{1}$ mutant embryo, pMad staining is strongly reduced.

Fig. 6. An activated Thick veins receptor can partially rescue the dorsal closure defects of *Sec61α*^{1}. (A) Confocal optical section of a non-rescued, $Sec61\alpha^{1}$/e22c-Gal4, $Sec61\alpha^{1}$ stage 17 embryo. Note that the dorsal surface is completely open and the brain (asterisk) and guts (arrow) are extruded. Arrowheads (in A-C) mark the anterior and posterior extent of the open dorsal surface. (B, C) Confocal optical sections of partially rescued, presumably $Sec61\alpha^{1}$/e22c-Gal4, $Sec61\alpha^{1}$;tkv^{QD}/+ embryos, showing the range of phenotypes observed. The weakest rescued embryos (B) showed a small dorsal hole with the brain and guts confined to the interior. Stronger rescue (C) resulted in a nearly completely enclosed embryo, with only a small gap where the lateral epidermal sheets were apposed but had not fused.

Fig. 7. Midgut morphogenesis is defective in *Sec61α* mutant embryos. Confocal optical sections of a stage 16 w^{1118} embryo (A), a stage 16 $Sec61\alpha^{1}$ mutant embryo (B) and a stage 17 $Sec61\alpha^{1}$/e22c-Gal4, $Sec61\alpha^{1}$;tkv^{QD}/+ embryo (C) stained with antibodies against Fasciclin III (Fas III). Note the four chambers of the midgut in w^{1118} embryo (asterisks) and the disorganized midguts in the $Sec61\alpha^{1}$ mutant embryos. The second midgut constriction is indicated by an arrow in panel A and is missing is $Sec61\alpha^{1}$ mutant embryos.

Supplemental Fig. 1. Most mid-embryonic morphogenetic events occur normally in *Sec61α* mutant embryos. Confocal optical sections of w^{1118} (A, C, and E) and $Sec61\alpha^{1}$ mutant (B, D, and F) embryos stained with antibodies against Neuroglian (A, B), Coracle (C, D), or Uninflatable (E, F). In all cases anterior is to the left. Wild type and mutant animals for each experiment were fixed and stained in parallel and imaged using identical settings. (A, B) The peripheral nervous system (a segmentally repeated unit is indicated by the arrow) is normally patterned in stage 14 $Sec61\alpha^{1}$ mutant embryos. (C, D) Salivary gland morphogenesis (dorsal and posterior migration of the gland) has occurred normally in stage 14 $Sec61\alpha^{1}$ mutant embryos as judged by Cor staining to visualize the gland. The salivary gland (arrow) occupies its normal position and has fully elongated towards the posterior. Note also that Cor is correctly localized to the apical lateral membrane (the region of the septate junction) in the mutant embryos. (E, F) Tracheal patterning is normal in stage 15 $Sec61\alpha^{1}$ mutant embryos, but the diameter of the tracheal tubes is smaller. The dorsal trunk is indicated by an arrow. The dorsal branches are notably present in $Sec61\alpha^{1}$ mutant embryos (indicated by arrowheads).

Table 1
Lethal-phase of *Sec61α* mutant and rescued animals

Genotype	% Embryonic lethality[a] (*n*)[b]	% Larval lethality[a] (*n*)[b]	% Pupal lethality[a] (*n*)[b]
Sec61α^{1}	100 (400)	N/A	
Sec61α^{1}*/Df(2L)BSC6*	100 (299)	N/A	
Sec61α^{1}*/Sec61α*^{k04917}	46 ± 6 (448)	100 (250)	
Sec61α^{k04917}	58 ± 8 (582)	100 (250)	
Sec61α^{1}*;P{Sec61α}*[c]	5 ± 1 (397)	37 ± 4 (376)	100 (237)
Sec61α^{1}*/Sec61α*^{k04917}*; P{Sec61α}* [c]	2 ± 3 (298)	22 ± 8 (292)	4 ± 3 (230)

[a] mean ± sd from three independent experiments
[b] total number of animals of indicated genotype that were scored
[c] genomic rescue construct line CM15-1

Table 2
tkv^{Q253D} rescue of $Sec61\alpha^{1}$ mutant animals

Cross	% $Sec61\alpha^{1}$ embryos showing DC rescue[a] (*n*)[b]
e22c-Gal4, Sec61α¹/CyO **X** *Sec61α¹/+; UAS-tkv^{Q253D}/+*	67 ± 6 (55)
T80-Gal4, Sec61α¹/CyO **X** *Sec61α¹/+; UAS-tkv^{Q253D}/+*	49 ± 5 (63)
322.3-Gal4, Sec61α¹/CyO **X** *Sec61α¹/+; UAS-tkv^{Q253D}/+*	45 ± 2 (329)
e22c-Gal4, Sec61α¹/CyO **X** *Sec61α¹/+; UAS-Dpp/+*	10 ± 3 (106)
T80-Gal4, Sec61α¹/CyO **X** *Sec61α¹/+; UAS- Dpp/+*	3 ± 3 (255)
322.3-Gal4, Sec61α¹/CyO **X** *Sec61α¹/+; UAS- Dp /+*	5 ± 3 (105)

[a] 16-20 hr AEL progeny of the indicated crosses were fixed and stained with antibodies against Coracle. Only *Sec61α¹* mutant animals stain at this stage. % DC rescue reflects the mean ± sd from three independent experiments. Note that maximal expected rescue is 50%.
[b] Total number of embryos that stained with Cor.

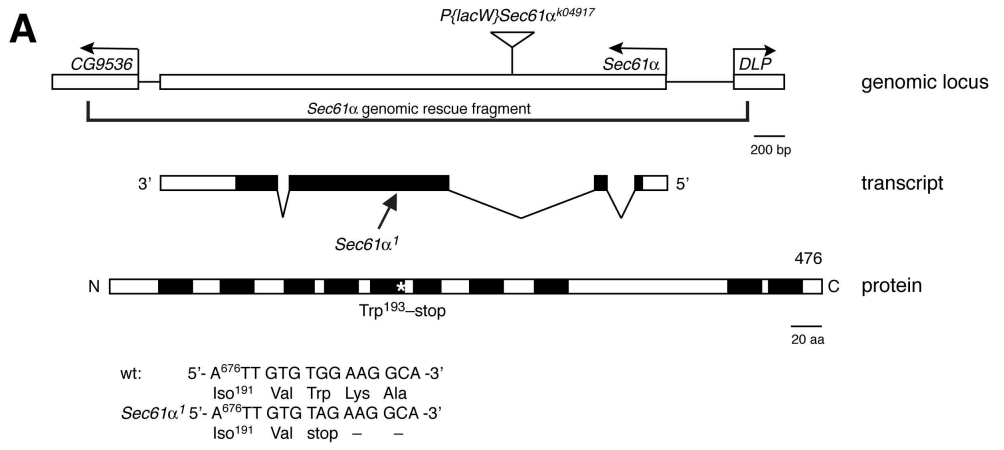

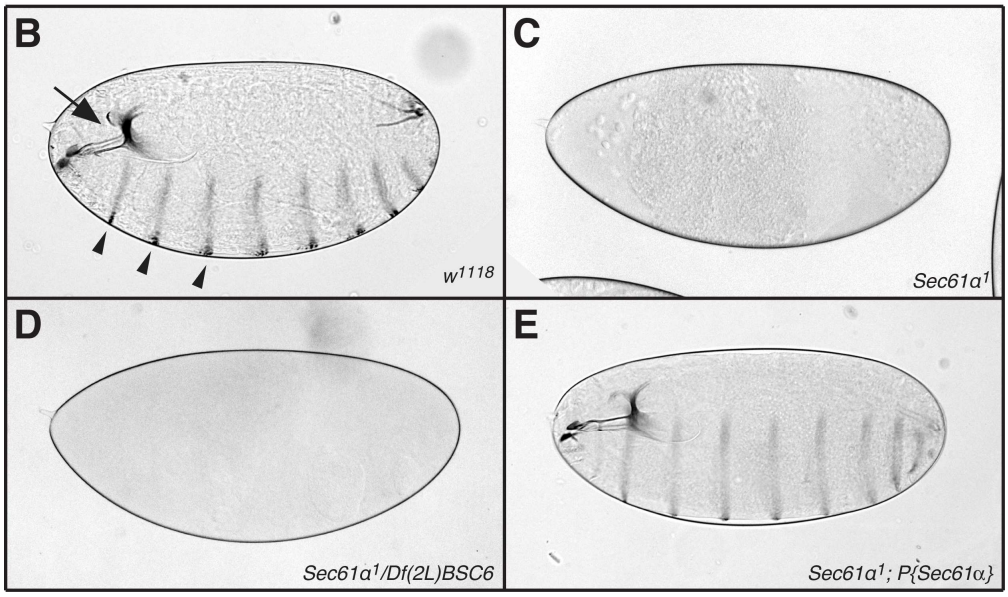

Fig. 1
212x239mm (300 x 300 DPI)

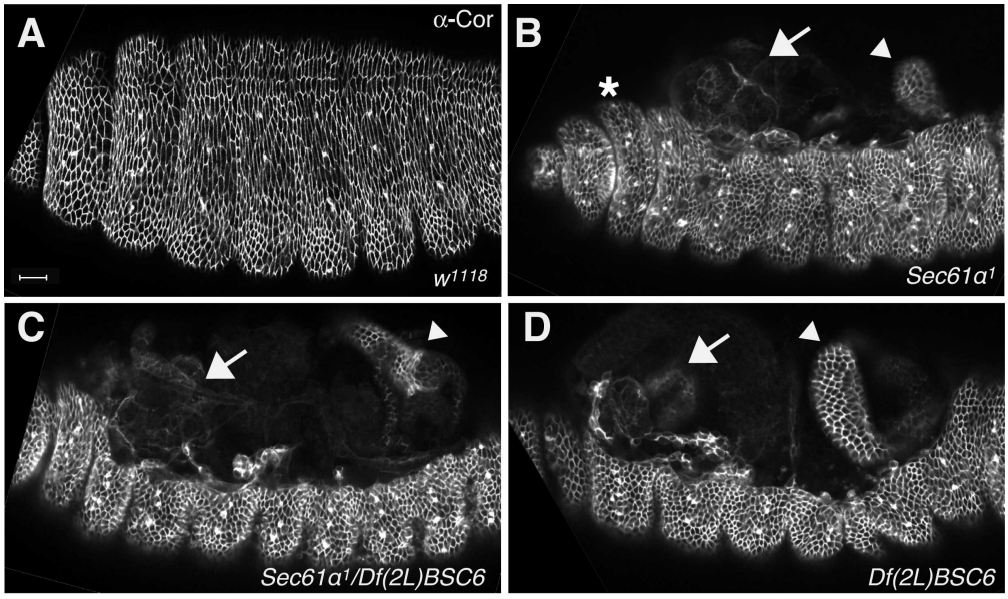

Fig. 2
209x123mm (300 x 300 DPI)

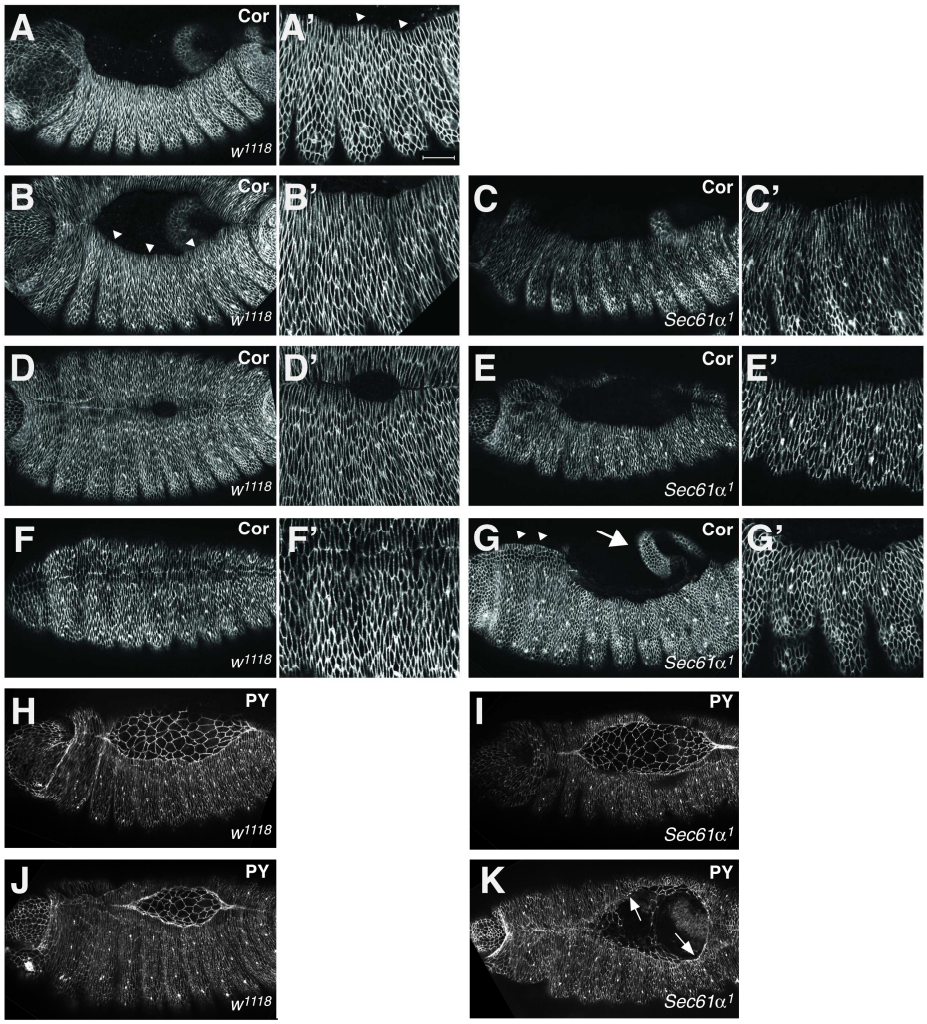

Fig. 3

215x279mm (300 x 300 DPI)

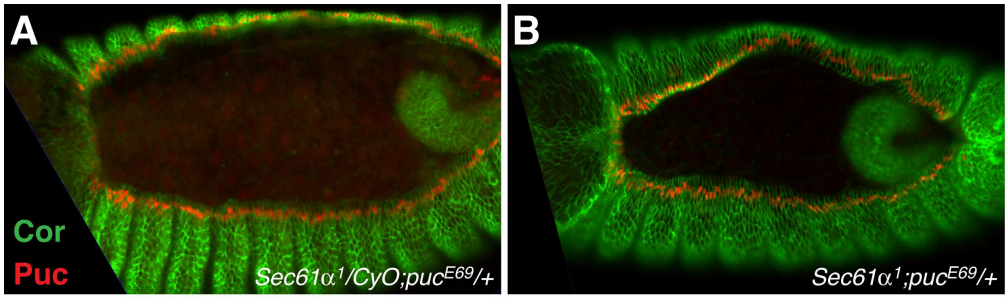

Fig. 4
209x62mm (300 x 300 DPI)

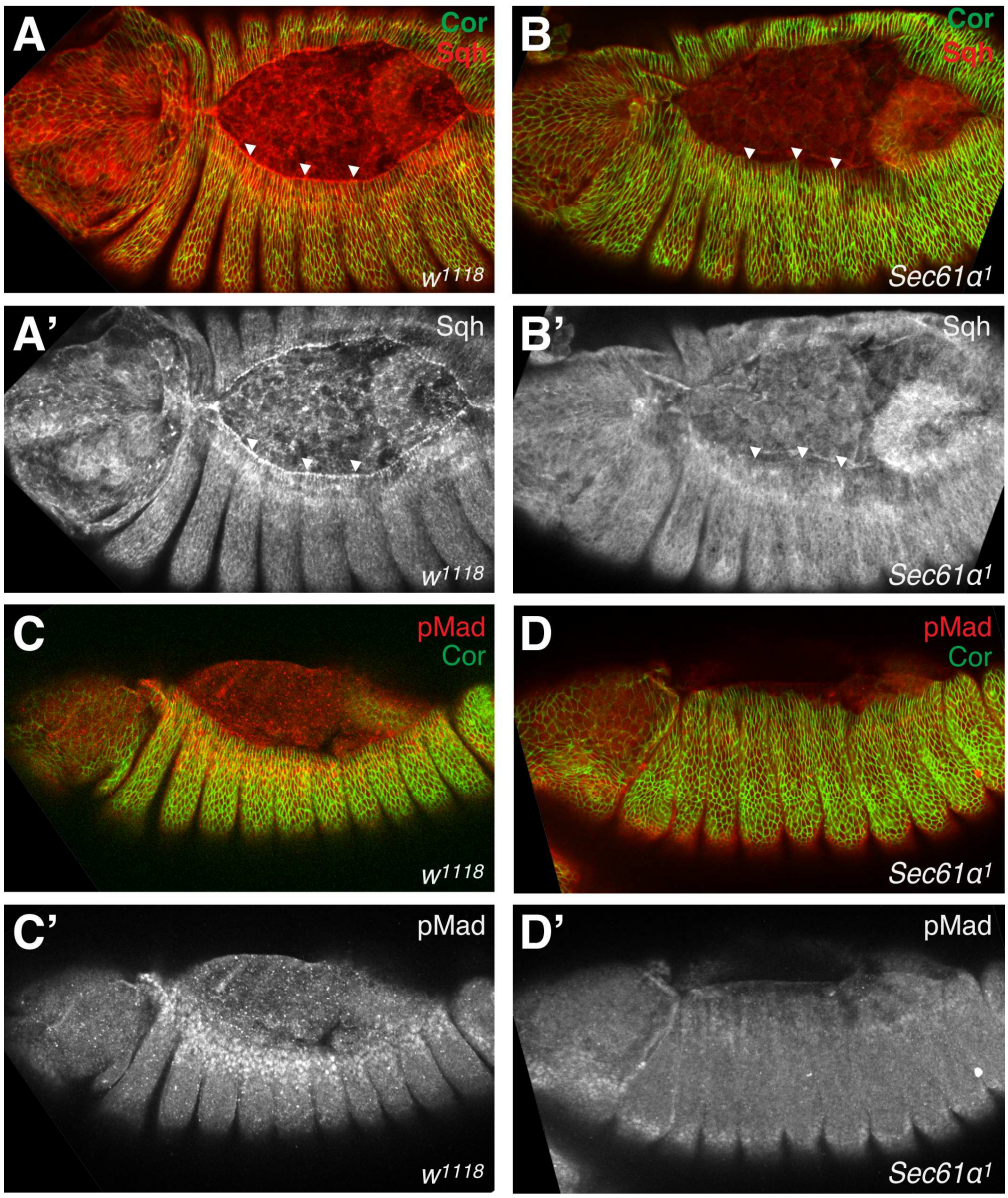

Fig. 5
180x214mm (300 x 300 DPI)

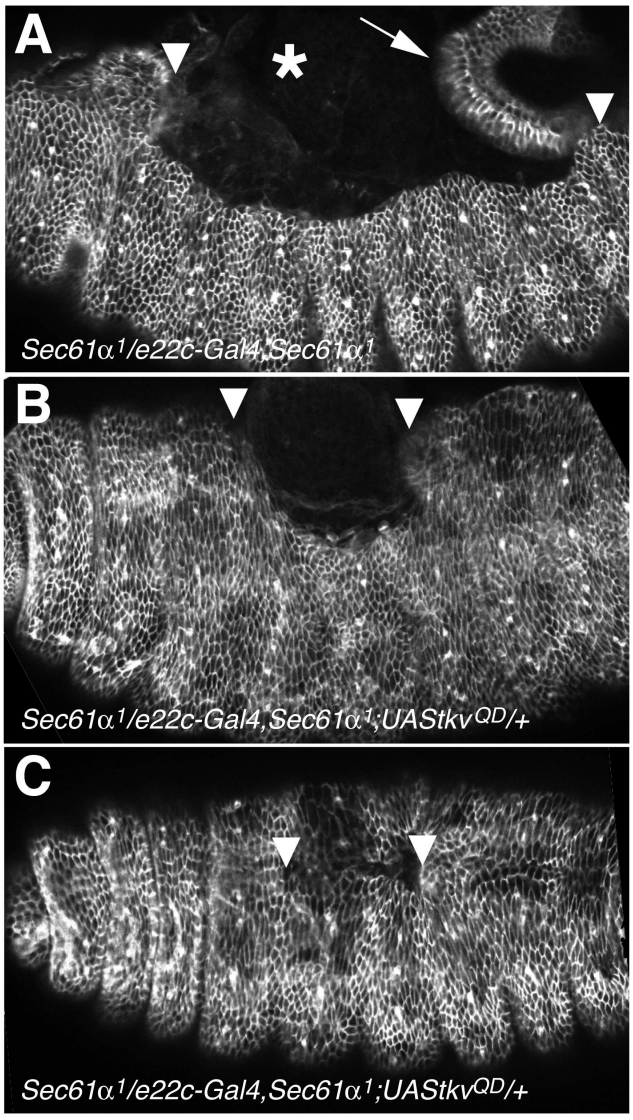

Fig. 6
215x279mm (300 x 300 DPI)

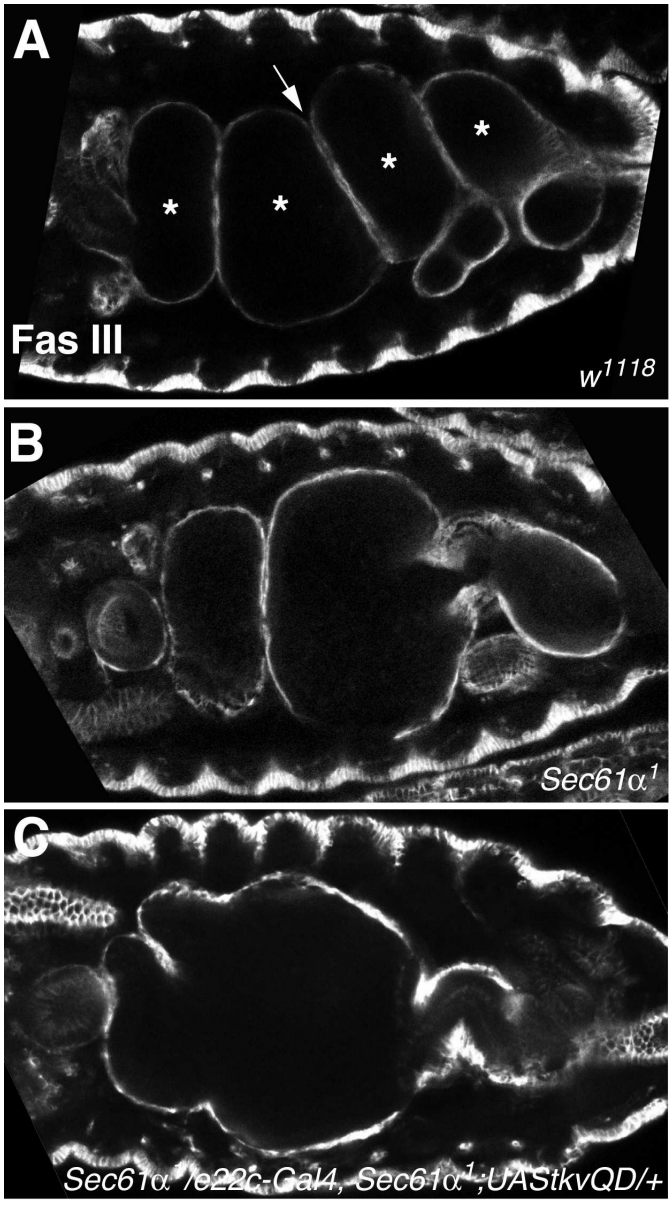

Fig. 7
105x189mm (300 x 300 DPI)

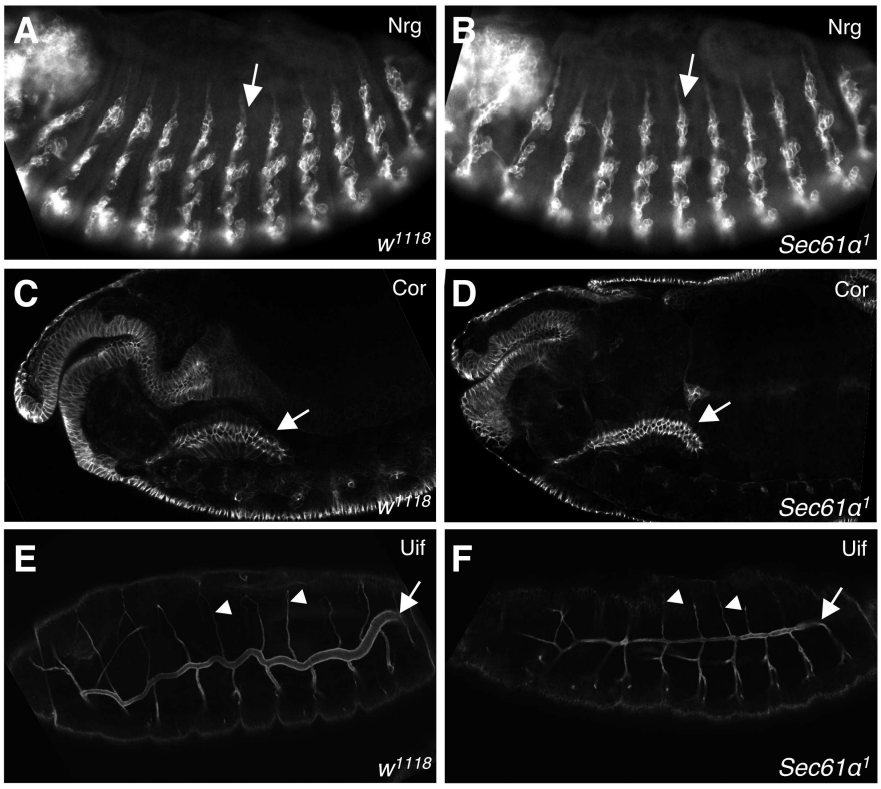

Supplemental Fig. 1
215x279mm (300 x 300 DPI)